Available online at www.sciencedirect.com
SCIENCE DIRECT®
ELSEVIER
Nuclear Instruments and Methods in Physics Research A 550 (2005) 551–558
NUCLEAR INSTRUMENTS & METHODS IN PHYSICS RESEARCH Section A
www.elsevier.com/locate/nima

Production of gas gaps for the Forward RPCs of the CMS experiment

S. Park[a], S.H. Ahn[a], S.Y. Bahk[b], B. Hong[a], S.J. Hong[a], M. Ito[a], T.I. Kang[a], B.I. Kim[a], J.H. Kim[a], M.J. Kim[a], T.J. Kim[a], Y.J. Kim[c], Y.U. Kim[d], D.G. Koo[e], K.B. Lee[a], K.S. Lee[a,*], S.J. Lee[f], J.K. Lim[a], D.H. Moon[a], S.K. Nam[g], W.J. Park[a], J.T. Rhee[h], M.S. Ryu[a], K.S. Sim[a]

[a]*Department of Physics and Korea Detector Laboratory, Korea University, Seoul 136-701, South Korea*
[b]*Department of Physics, Wonkwang University, Iksan 570-749, South Korea*
[c]*Department of Physics, Cheju National University, Cheju 690-756, South Korea*
[d]*Department of Physics, Chungbuk National University, Chungjoo 361-763, South Korea*
[e]*Department of Physics, Seoul National University of Education, Seoul 137-742, South Korea*
[f]*Department of Biomedical Engineering, Seonam University, Namwon 590-711, South Korea*
[g]*Department of Physics, Kangwon National University, Chunchon 200-701, South Korea*
[h]*Institute for Advanced Physics, Konkuk University, Seoul 143-701, South Korea*

Received 7 December 2004; received in revised form 4 May 2005; accepted 9 May 2005
Available online 6 July 2005

Abstract

The production of gas gaps, the core components of the Forward RPCs in the CMS experiment, has reached a mature stage of the production stream. A total of 360 gas gaps, equivalent to 120 RPCs, has been manufactured, tested for quality control, and delivered to CERN in Switzerland and to Pakistan, where the complete Forward RPCs are being assembled. In this paper, the layout of the gas gaps, the production procedures, facilities, and the selection process of the qualified gas gaps are presented.

Keywords: Compact muon solenoid; Forward RPCs; Muon trigger; Aging effect; Gas gap; Linseed oil coating; Silk screen method

1. Introduction

The role of resistive plate chambers (RPCs) in the CMS experiment is to trigger muons and classify their momenta, ranging from a few GeV/c to 1 TeV/c. The RPCs for the forward region of

*Corresponding author. Tel.: +822 3290 4277.
E-mail address: kslee0421@korea.ac.kr (K.S. Lee).

0168-9002/$ - see front matter
doi:10.1016/j.nima.2005.05.052

CMS covers a pseudo-rapidity ranging from 0.92 to 2.1, as shown in Fig. 1 for a quadrant of the CMS detector [1].

Important parameters to determine the geometrical layout and the mechanical details for the gas gaps, which are the core components of the RPCs, must be chosen with the consideration of the geometrical coverage of the trigger, spurious noise rates, the electric and long-term stability against aging. The expected detection rate of background particles, such as gamma rays and neutrons induced by the beam, reaches as much as $300\,\mathrm{Hz/cm^2}$ [1]. The relatively large current per unit area of the detector would be consistently drawn during the long-term operation of the CMS detector. In such experimental environment, the preservation of the initial detector characteristics is the key factor to determine the mechanical details of the gas gaps and their production method.

In October 2002, the Engineering Design Review (EDR) committee of the CMS experiment decided to apply an additional linseed oil coating to the gas gaps for the Forward RPCs in the pseudo-rapidity region, $\eta < 1.6$. Comparison test results for the oiled and non-oiled RPCs, performed at the Gamma Irradiation Facility (GIF) at CERN in August 2003, clearly showed a large reduction of spurious noise in virtue of the linseed oil coating [2]. The typical noise rate of the oil-treated RPC is less than $5\,\mathrm{Hz/cm^2}$, while the noise rate of the RPCs made of plane bakelite is as much as $50\,\mathrm{Hz/cm^2}$.

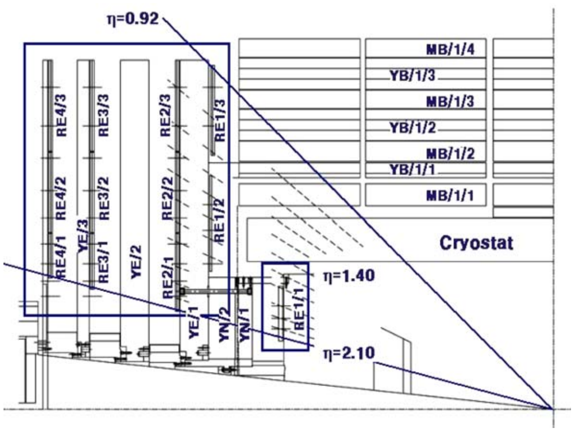

Fig. 1. Schematic view of a quadrant of the CMS detector. The Forward RPCs trigger particles in the pseudo-rapidity η ranging from 0.92 and 2.1.

For the further study of the oiled Forward RPCs, a long period test to observe aging phenomena is being performed using a 200 mCi ^{137}Cs gamma ray source [3]. Four double gap, RPCs with a size of $40\,\mathrm{cm} \times 40\,\mathrm{cm}$ were manufactured for the test. The preliminary result shows that the gamma ray irradiation for 75 days, induced an amount of integrated charge of $\sim 0.16\,\mathrm{C/cm^2/gap}$ in the gas gaps, which is equivalent to the expected amount induced by about 3 years of detector operation. No significant aging effect has been observed, as yet.

2. Layout of gaps for Forward RPCs

The Forward RPC system consists of four RPC Endcap (RE) stations designated RE1, RE2, RE3, and RE4, as shown in Fig. 1. Each RE station is divided into three detector segmentations along the radial direction in the cylindrical symmetry of the CMS detector. The three segmentations are labelled $\mathrm{RE}*/1$, $\mathrm{RE}*/2$, and $\mathrm{RE}*/3$ for each RE station, sequentially ordered from the detector center ($r = 0$), where '$*$' represents the RE station numbers being 1, 2, 3, or 4.

All the Forward RPCs have a trapezoidal shape. The size of each ϕ sector of the muon trigger is $\Delta\phi = \frac{5}{16}^\circ$ [1]. The 10° RPCs equipping the region of $\eta < 1.6$ ($\mathrm{RE}*/2$ and $\mathrm{RE}*/3$) cover 32 ϕ sectors and are segmented into three along r. The 20° RPCs in $1.6 < \eta < 2.1$ cover 64 ϕ sectors and are segmented into four along r ($\mathrm{RE}*/1$).

Each double gap RPC [4,5] consists of two layers of gas gaps. The top layer is divided into two gas gaps to allow signal extraction from the strips placed between the two layers. The diagram for the layout of gaps in the Forward RPCs is shown in Fig. 2.

Fig. 3 shows the cross-section diagram of a gas gap. The bakelite sheets of 2 mm thickness were delivered from Italy. The quality control procedures for the bakelite sheets, which include checking the resistivity, the cutting, and the chemical treatment were performed in Italy, before

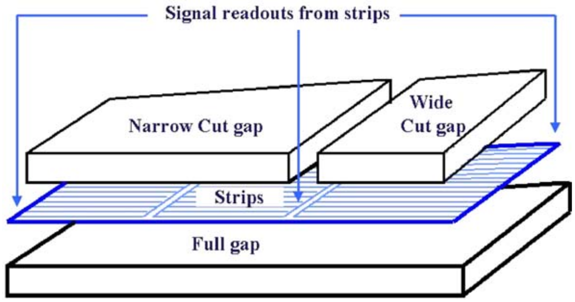

Fig. 2. Layout of gaps in a double-gap Forward RPC. The top layer is divided into two gas gaps to allow for signal readout from the segmented strips placed between the two layers.

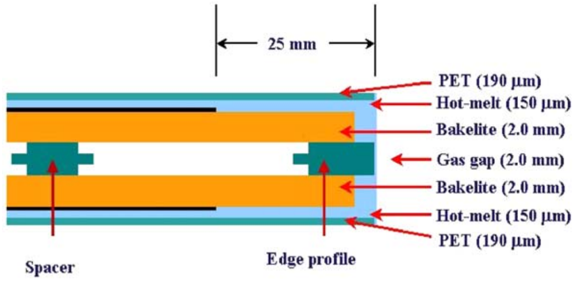

Fig. 3. Cross-section diagram of a gas gap.

transportation to Korea. Coin-shaped spacers maintain the uniform thickness of the gas volume. They were made of polycarbonate for which the bonding strength with epoxy resin is excellent. Edge profiles along the periphery of the gas gap for gas sealing and block components of gas inlets and outlets were also made of polycabonate for the same reason. The mechanical tolerances in thickness of the spacers and edge profiles are ±10 and ±30 µm, respectively. Fig. 4 shows the diagrams for these three gap components.

3. Production procedures

The important design parameters for the production facilities depend on the mechanical uniformity and the electrical stability of the gas gaps. In addition, the maintenance of initial detector characteristics for the long-term CMS operation

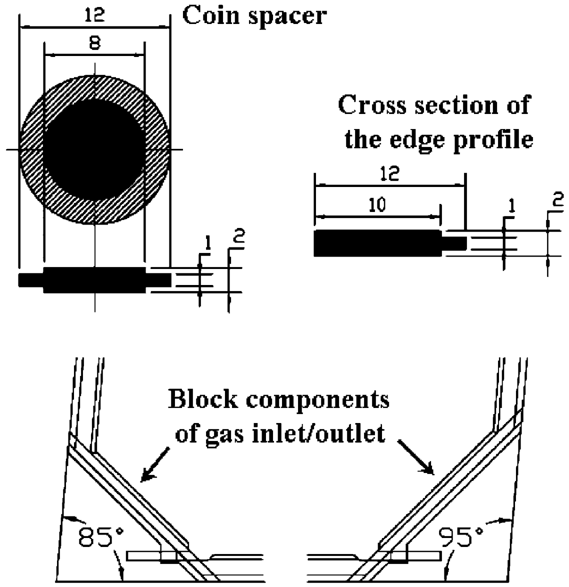

Fig. 4. Designs of coin-shaped spacers (top left), gap edge profiles, (top right), and block components of gas inlets and outlets (bottom). The diagram at the bottom shows the geometrical matching of the block components to the corners of gaps with two different angles.

was also an important factor to be considered for the preparation of the production facilities.

Before the assembly of gas gaps, a thin carbon layer and an insulator sheet are coated on the bakelite sheets. The procedure of oil coating is done after the gas gaps are assembled. The final stage of the production consists in the tests for the quality control.

Thin carbon layers both on the high voltage and on the ground sides of gas gaps are coated by a silk screen method. The surface resistivity of the carbon surfaces is controlled by a 20 µm thick silk screen mesh. The surface resistivity of the carbon layer ranges from 100 to 250 kΩ/□ after being dried for 5 days. The silk screen method for the graphite coating is relatively fast for mass production, and shows to be effective to control the uniformity of the surface resistivity. The operation table and the accessories are shown in Fig. 5.

The carbon layers of the gas gaps are electrically protected by a 190 µm thick polyester (PET) sheet. Adhesive based on ethylene vinyl acetate (EVA) is used to glue the PET film on the graphite-coated

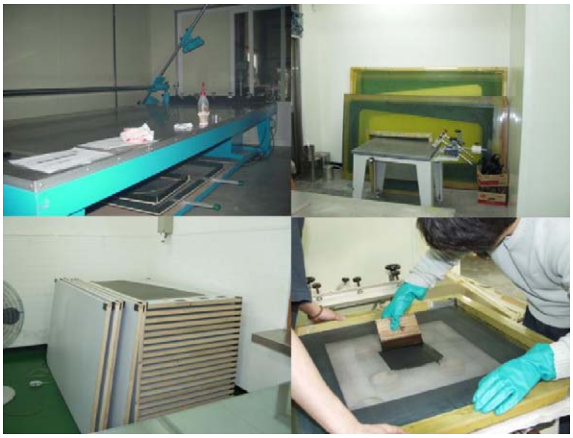

Fig. 5. Silk screen table and the accessories for the graphite coating. The coating area and the thinness of the carbon layer are controlled by the silk mesh (upper right). The multi-layer shelves (lower left) allow for the drying of the carbon layers for many gaps in parallel. A few samples were made to monitor the variation of the surface resistivity as a function of time (lower right).

bakelite sheet. The thin film of the 'hot' adhesive is extruded through a long 500 μm wide slit, and is immediately dispensed over the carbon-coated bakelite surface. The PET film is immediately placed on the hot glue surface and then pressed by an air-pressure loaded roller. The thickness of the thin adhesive after hardening is $160 \pm 20\,\mu m$. Fig. 6 shows the extrusion facility and the control device of the PET film coating.

Three flat metric tables, rubber chambers for pressurization, specially machined jigs to fix the spacers and the peripheries are used to assemble the gas gaps. The facility was designed and manufactured to enable three consecutive assemblies using three sets of flat metric tables and rubber chambers (Fig. 7). Coin-shaped spacers and edge profiles, supporting a gas gap, are properly grinded to maximize the bonding strength with epoxy. Positioning of the spacers is guided by special jigs made out of 5 mm thick plexiglass plates, where holes of 13 mm diameter were machined in the exact positions of the spacers. The edge profiles, running along the periphery for the gas sealing, are also fixed by jigs that were machined out of 6 mm thick aluminum plates.

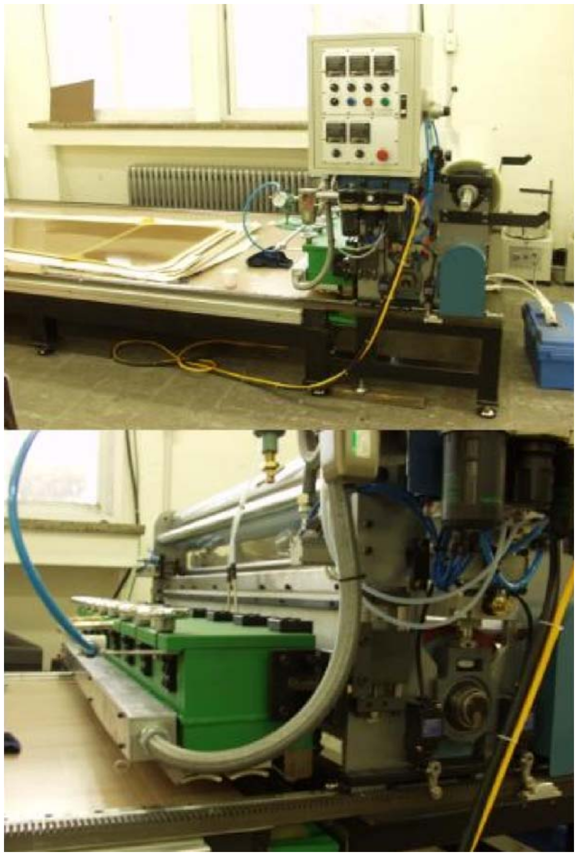

Fig. 6. The PET film coating facility for the protection of the carbon layers. A thin film of the hot adhesive is extruded through a 500 μm wide slit of the extrusion tank shown in the lower part of the figure.

Each flat metric table, where a few sets of gas gaps can be assembled, slides into a chamber for epoxy curing. The maximum working time for the epoxy is 60 min, and the glue curing time to get the full hardening is approximately 24 h at 25 °C. During the glue curing time, an air-loaded rubber chamber uniformly applies a positive pressure of 20 hPa over the whole surface of the gas gaps and the metric table.

The application of the linseed oil coating to the Forward RPCs has been successful to reduce a large fraction of the spurious noise in the avalanche mode operation. However, the serious question for the oiled RPCs is whether the initial RPC characteristics, such as current, noise rate, or

Fig. 7. Facility for the assembly of gas gaps. The facility equipped with three sets of flat metric tables and rubber chambers enables three consecutive assembly procedures.

rate capability can be sustained for the long-term detector operation. The complete polymerization of the linseed oil layer, coated inside the gas gap, would ensure the reliability of the long-term operation.

The oil coating facility, shown in Fig. 8, consists of two oil tanks, one lifting device, two air pumps, one air compressor, and a press device which vertically holds the gas gaps both during the oil coating and the air drying. The lifting device, holding a 200 l oil tank, moves up vertically with a constant speed of 2 cm per minute. The lifting device hydrostatically injects the oil into the gas gaps which were mounted vertically in the pressing device. The air pump applies approximately 100 hPa to the gas gaps from outside to keep the pressure below 1 atm even after the oil is fully loaded. As the lifting device is lowered, a thin linseed oil layer automatically remains over the inside surfaces of the gas gaps. The thickness of the oil layer is 3–5 μm.

Right after the drain and suction of the linseed oil from the gas gaps, air with relative humidity of 40% is applied to polymerize the oil layers. The flow rate applied per a gas gap ranges from 70 to 100 l/h. The period of applying the air flow ranges from 40 to 60 h. The flow rate and its period depend on the size of the gap. The addition of humidity to the air is important to avoid any

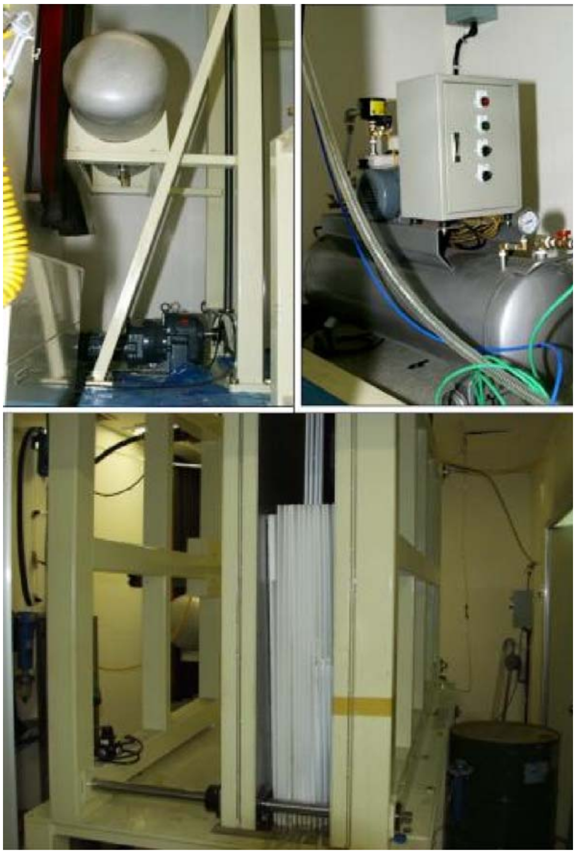

Fig. 8. Oil coating facility. The 200 l oil tank and the lifting device are shown in the upper left of the figure. The pressure inside the gas gaps and the movement of the oil tank are controlled at the control panel (upper right). Before oiling, the gas gaps are vertically mounted inside a pressing device, as shown in the lower picture.

deformation of the gas gaps due to the drying process. The test results for a few samples, produced by this oil coating facility, to check the polymerization of the oil layer were satisfactory.

4. Quality control

For the quality control of the gas gaps, two tests are performed: the first one includes checking for gas tightness and failures of spacer bonding for each gas gap. The second step of the quality control consists in the measurements of the current values of the gas gaps at several high-voltage settings.

To search for gas leaks and failures of spacer bondings, an over-pressure of 20 hPa is slowly applied to each gap placed on the flat metric table. For a gas gap to be qualified, the loss of the applied pressure should be less than 0.2 hPa over a 15 min period. In addition, no failure of a spacer bonding is accepted with the presence of 20 hPa over-pressure. The gas gaps, showing significant gas leaks, are fixed by dispensing epoxy on the leak positions. Roughly 5% of the assembled gas gaps were rejected due to the failure of a spacer bonding or a misalignment of the block component for gas in/outlets, which causes serious gas leaks.

The measurement of the chamber currents provides the acceptance criterium for qualified gas gaps at the initial stage of the detector operation. The gas mixture for this high-voltage test is 96.5% tetraflouroethane ($C_2H_2F_4$) and 3.5% i-C_4H_{10}. An amount of the mixed gas, equivalent to roughly 15 times the detector volume, is circulated through the gas gaps before applying the high voltage.

At the beginning of the test, the high voltage applied to the gas gaps is set to 2 kV to check any disconnection or electrical shortage. Then, the high voltage is raised to 8.5 kV with 1 kV steps over 5 h. The high voltage is then kept at 8.5 kV, the beginning of the gas avalanche, for 12 h to observe the behavior of the ohmic dark currents of the gas gaps. The high voltage is then increased with steps of 100 V from 8.5 to 9.4 kV. The expected high-voltage value to obtain a 95% detection efficiency at 1013 hPa is 9.1 kV with the gas mixture of 96.5% $C_2H_2F_4$ and 3.5% i-C_4H_{10}. The high voltage for the gas gaps is kept at 9.4 kV for 36 h to monitor the current behavior at the operation voltage. Due to the tight production schedule the maximum length of the high voltage test, including the gas circulation, is limited to 5 days for each gap. The acceptance criteria for the currents of qualified RE2/2 gas gaps are shown in Table 1.

The current values of the gas gaps were recorded at four high voltages, 8.5, 9.0, 9.4, and 9.6 kV, together with the temperature, the humidity, and

Fig. 9. Facilities for the high-voltage test. As shown in the left part of the figure, three high voltage supplies, four 12-channel current measurement devices, and a 6-channel gas supply system are used for the high-voltage test. The right part of the figure shows 22 RE2/2 full gas gaps, placed on multi-layer shelves, for the test. After completing the high-voltage test, a bar code is assigned to each gas gap for later tracking.

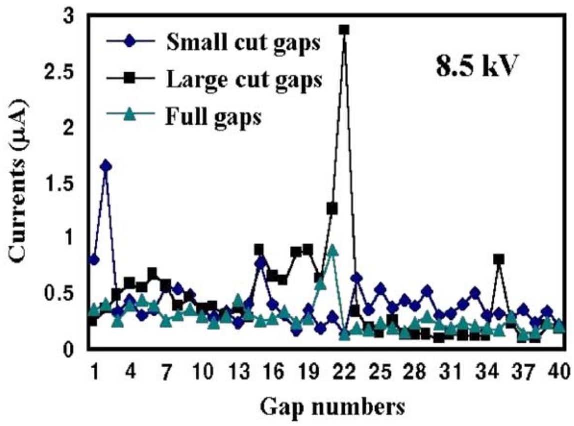

Fig. 10. Current values of 120 qualified RE2/2 gas gaps at 8.5 kV.

Table 1
The current limits at 8.5 and 9.4 kV for qualified RE2/2 gas gaps

	8.5 kV (μA)	9.4 kV (μA)
Small cut gaps	2.0	3.0
Large cut gaps	3.0	5.0
Full gaps	5.0	8.0

the pressure. Fig. 9 shows the facilities for the high-voltage test and 22 RE2/2 full gas gaps, placed on multi-layer shelves, for the test. The current values of 120 qualified RE2/2 gas gaps at 8.5 and 9.4 kV are shown in Figs. 10 and 11, respectively.

5. Packing and transportations

Every 60 qualified gas gaps, equivalent to 20 RPCs, are vertically mounted into a wooden box (Fig. 12), equipped with four pre-loaded bars which were designed to horizontally press the surface of the gas gaps. Five-mm thick polystyrene foam sheets are placed between the layers of the gas gaps to absorb shocks which could be caused during the transportation. An extra protection from humidity is provided by wrapping the whole 60 gas gaps with thin vinyl film.

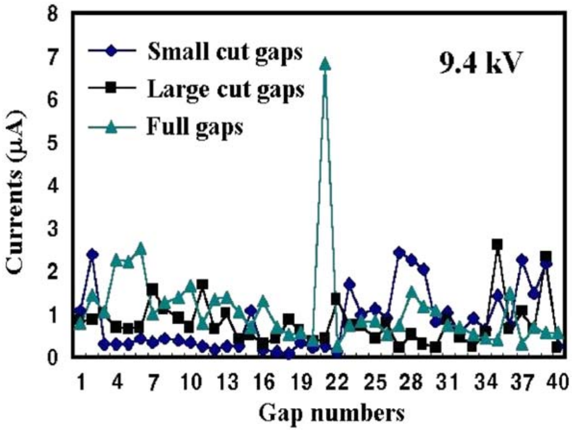

Fig. 11. Current values of 120 qualified RE2/2 gas gaps at 9.4 kV.

The pipes for the gas inlets and outlets are left open to adapt to sudden variations of pressure during air-transportation. At the beginning of the departures of airplanes, the maximum rate of the variation in the atmospheric pressure is expected to be 30 hPa/min. Therefore, the choice for the safest transportation is to allow for free air flow through the gas pipes.

6. Conclusions

The mass productions of the gas gaps and the quality control tests for the Forward RPC system have reached the maximum productivity. The yield to produce qualified gas gaps is now above 80% of the qualified bakelite sheets provided by Italy.

The production and transportation of the gas gaps were completed for the RE1/2, RE1/3, and RE2/2 RPCs by October 2004. The further

Fig. 12. Wooden boxes, equipped with four pre-loaded bars, specially designed for safe transportation of the gas gaps. The boxes are also used to ship the qualified bakelite sheets from Italy to Korea via CERN.

production for the Forward RPCs of CMS is reliably on schedule.

Acknowledgements

This work was supported by the Ministry of Science and Technology, Republic of Korea, by the Korean Science and Engineering Foundations under Grant No. R0404621, and by Wonkwang University in 2003.

References

[1] The Muon Project, Technical Design Report, CERN/LHCC 97-32, Dec. 1997.
[2] S. Park, et al., Nucl. Instr. and Meth. A 533 (2004) 37.
[3] S. Park, et al., Talk given in Korea Physical Society meeting, April 2004.
[4] S. Park, et al., Nucl. Instr. and Meth. A 456 (2000) 29; S. Park, et al., Nucl. Instr. and Meth. A 443 (2000) 31.
[5] B. Hong, et al., Nucl. Instr. and Meth. A 533 (2004) 32; B. Hong, et al., Nucl. Instr. and Meth. A 469 (2001) 323.